PARAMETRIC STUDY ON LATERAL STIFFNESS OF PARTIALLY BONDED RUBBER PAD ISOLATORS: INFLUENCE OF ASPECT RATIO AND BIDIRECTIONAL LOADING

Md. Mistak Hossain[1], Md Nahis Uddin Bhuiyan Nid*[2]

[1]*Graduate Student, North South University, Bangladesh, e-mail: mdmistakabir786@gmail.com*
[2]*B.Sc. Graduate, Chittagong University of Engineering and Technology, Bangladesh, e-mail: nahisnid@gmail.com*

***Corresponding Author**

ABSTRACT

The lateral stiffness of square shaped Scrap Tire Rubber Pad (STRP) base isolators under bidirectional cyclic loading is examined in this study in relation to aspect ratio and bonded area %. Five isolator sizes, ranging from 24mm x 24mm x 24 mm to 72mm x 72mm x 24 mm, were evaluated; each corresponded to a distinct plan-size-to-thickness aspect ratio. To replicate partial bonding situations, bonding levels were changed from 0% to 100%. For remote or rural locations or seismically active sites, scrap tire rubber pad base isolators constructed from recycled tires offer an affordable and environmentally responsible substitute. AR-3 shows the highest lateral stiffness of 639.3 KN/m for 100% bonded at 45 degree loading and AR-1 shows the lowest value of 35.78 KN/m. This lateral stiffness increases with increasing of aspect ratio. Aspect ratio and bonding configuration critically affect the lateral load resistance of low-cost STRP isolators, with the AR-3 isolator proving the most effective and stable for seismic protection.

Keywords: *Lateral Stiffness, Seismic Protection, Isolators.*

1. INTRODUCTION

Due to budgetary constraints, seismic design techniques are frequently disregarded in the planning and construction of low- to medium-rise structures in developing nations. As a result, many buildings are susceptible to earthquakes, which can cause severe damage to infrastructure and fatalities. In fact, several anti-seismic concepts and design standards have led to new ideas and design techniques to reduce seismic damage and enhance a structure's resilience to earthquakes. Installing base isolators between the superstructure and foundation, which reduce the structure's seismic demand during an earthquake, is one of the most extensively used techniques (Nishi et al., 2019). Because of their excellent seismic performance and longevity, steel-reinforced elastomeric isolators (SREIs) are among the most widely used base isolator types. However, as noted by (Pan et al., 2005), the problem with SREIs is their high production costs and intricate manufacturing methods, which make them prohibitive for low-cost and non-commercial structures, especially in developing nations.

Recent research and development efforts have focused on creative, affordable seismic-isolation technologies ideal for poor nations. The use of locally accessible or recycled materials, lowering production costs and energy usage, and streamlining design and installation procedures are among the goals of current development. Scrap tyre rubber pad (STRP) isolators, which are made from recycled car tyres, are an economical and environmentally responsible way to provide seismic isolation. STRP isolators are particularly suitable for use in developing and impoverished nations due to their straightforward setup and installation (Kelly, 1999) (Mishra, 2012) (Zisan & Igarashi, 2021). In addition to lowering production costs, the use of recycled materials reduces the environmental impact of the estimated 1.5 billion tyres accumulated worldwide each year (Mashiri et al., 2015). Furthermore, it is asserted that STRP isolators are an affordable way to mitigate earthquakes while also reducing waste and protecting the environment. Mishra found that STRP isolators performed well in a pseudo-dynamic test for medium- to low-rise buildings (Mishra, 2012). Zisan and Igarashi (Zisan & Igarashi, 2021) and Hossain et al. (Hossain et al., 2024) examined the force-displacement relationship and lateral performance of unbonded square and strip-shaped STRP isolators in further studies. Additionally, they discussed how the length-to-width ratio, bearing height, and loading direction may affect the horizontal stiffness and seismic demand of unbonded STRP isolators. Hossain (Hossain et al., 2024) showed that for different bonded portion with two different loading direction fluctuate the stiffness value. Prior research has mostly concentrated on the global lateral stiffness of structural members under lateral loads, connection details, or material characteristics. But in large scale numerically and experimental investigations have remained scarce. Specifically, aspect ratios of 1, 1.5, 2, 2.5, and 3 have not been thoroughly studied in order to determine the best configuration for maximum lateral stiffness for different loading direction. In order to close this gap, a parametric experimental study was carried out to measure the impact of aspect ratio on lateral stiffness. This experiment examined the horizontal stiffness of isolators of different sizes that were unbonded, moderately bonded, and fully bonded. For this experiment, size of isolator has been started from 24mm x 24mm x 24mm to 72mm x 72mm x 24mm square based base isolator for six different loading direction from 0° to 75° with a 15° interval between each. The stability of the STRP isolators in respect to various aspect ratios investigated in this study, which also identified the ideal design configuration.

2. METHODOLOGY

This effort includes material modelling, model creation, and model verification in addition to finite element analysis. Each methodological part is thoroughly explained in the flowing chapter.

2.1 Modelling of Materials

Similar to how a steel-reinforced elastomeric isolator is manufactured, an automobile tire is made by vulcanizing rubber with steel cord. The procedure of creating a rubber pad from used tires is shown in Figure 1 (Mishra, 2012). A scrap tire rubber pad made from a Bridgestone 385/65R22.5 tire has a thickness of 12 mm and five reinforcing layers that are orientated at an angle of ±70° with respect to

the carcass steel direction, as shown in Table 2, individual 12 mm rubber pads were adhered in a layered pattern to create the STRP isolator. Table 2 detail with the characteristics of the steel cable and scrap tire used in STRP isolators, which come from Bridgestone 385/65R22.5. In Table 3, it has shown detail of Aspect ratio with their bonded portion. The Mooney-Rivlin model is used in rubber modelling to precisely characterize the nonlinear elastic behaviour of rubber. Mishra (Mishra, 2012) estimated the hyper-elastic material constants for the three-term Mooney-Rivlin energy function using uniaxial testing. The rubber material constants are listed in Table 1. The idea of Aspect ratio is mainly ratio between length to height.

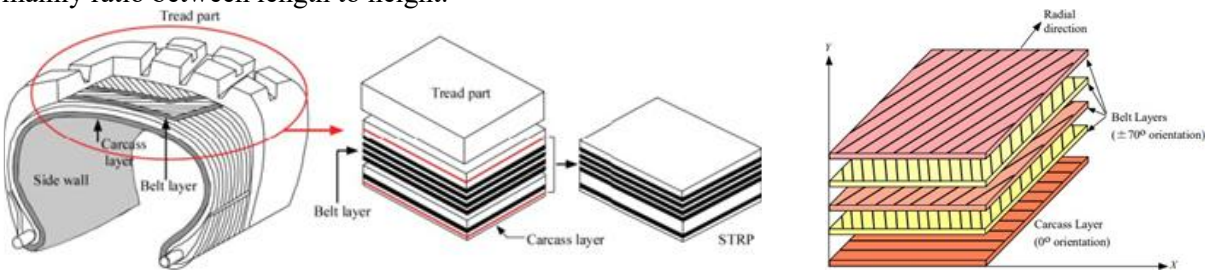

(a) (b)

Figure 1: STRP isolator: (a) Fabrication of STRP specimen; (b) Arrangement of steel reinforcing cords

Table 1: Mooney-Rivlin constants (Mishra, 2012)

C_{10}	C_{01}	C_{11}
0.40	1.22315	0.18759

Table 2: Properties of reinforcing steel cord in a STRP isolator (Igarashi & Zisan, 2021) (Hossain et al., 2024)

Layer	Poisson's ratio,υ	No. of filament	Filament dia (mm)	Steel cord area (mm^2)	Angle	Equivalent Thickness *tf* (mm)	Yield strength (GPa)	Modulus of elasticity *E*, (GPa)
Carcass	0.3	5	0.2	0.44	0°	0.40	2800	200
Belt	0.3	14	0.4	0.63	±70°	0.40	2800	200

Table 3: Bonded portion according to Aspect Ratio

Model	Aspect Ratio	Dimensions	Bonded Portion (%)	Bonded Area
STRP-0	1.0	24 × 24 × 24	0	0 × 0
STRP-25			25	12 × 12
STRP-50			50	17 × 17
STRP-75			75	21 × 21
STRP-100			100	24 × 24
STRP-0	1.5	36 × 36 × 24	0	0 × 0
STRP-25			25	18 × 18
STRP-50			50	25.5 × 25.5
STRP-75			75	31.2 × 31.2
STRP-100			100	36 × 36
STRP-0	2.0	48 × 48 × 24	0	0 × 0
STRP-25			25	24 × 24
STRP-50			50	34 × 34
STRP-75			75	41.6 × 41.6

STRP-100			100	48 × 48
STRP-0	2.5	60 × 60 × 24	0	0 × 0
STRP-25			25	30 × 30
STRP-50			50	42.5 × 42.5
STRP-75			75	52 × 52
STRP-100			100	60 × 60
STRP-0	3.0	72 × 72 × 24	0	0 × 0
STRP-25			25	36 × 36
STRP-50			50	51 × 51
STRP-75			75	62 × 62
STRP-100			100	72 × 72

2.2 Developing Models

Marc-Mentat software is used to model the STRP isolator using finite elements (Marc, 2018). Rubber material is modelled using an isoperimetric hexahedral element of the Herrmann type. Compared to higher-order elements, this element is favoured for contact analysis and modelling large deformations. In Figure 2, here shows bonded potion of STRP. A hollow isoperimetric rebar element is used to mimic the steel strands that reinforce the rubber composite. The steel cord layers, referred to as the carcass and belts 1 through 4, are arranged sequentially in Figure 3 (a). The rubber matrix materials are shown by the rebar elements inserted in the matching solid host components. Two 12 mm rubber-steel composites are designated as L1 and L2, respectively. A 24 mm STRP composite is produced by geometrically placing and superimposing L2 on L1. A bonded connection is used to model the contact between L1 and L2. Two additional pieces with appropriate dimensions are taken into consideration at the top and bottom faces of the isolator in order to replicate partial bonding between the STRP isolator and the surfaces of structural elements. They are called "Bonded-Top" and "Bonded-Bottom" which shows in Figure 2. Rigid planes are used to model these contact surfaces. The finite element models of steel chords and STRP isolators with fine mesh are displayed in Figures 3(a) and 3(b), respectively. A static axial load of 5 MPa is applied to each model's top surface. A complete finite element model with all boundary conditions is displayed in Figure 3(a). As illustrated in Fig. 3(d), the cyclic lateral displacement consists of six cycles, or shear displacements of 25%, 50%, 100%, 150%, 200%, and 250%. This lateral displacement is separated into two components based on the orientation of the displacement and then applied in two orthogonal directions of the isolator. In relation to the orthogonal direction, these components are aligned from 0° to 75° at intervals of 15°. Finding horizontal stiffness according to their Aspect ratio is the main goal for this work. The contact between rubber elements and bonded portions, as well as between building components and bonded parts, is thought to be glued, whereas the contact between the unbonded portion of the isolator and building components is meant to be a touched connection. A friction coefficient of 0.8 is considered for touch connections (Zisan & Igarashi, 2021) (Zisan & Igarashi, 2022).

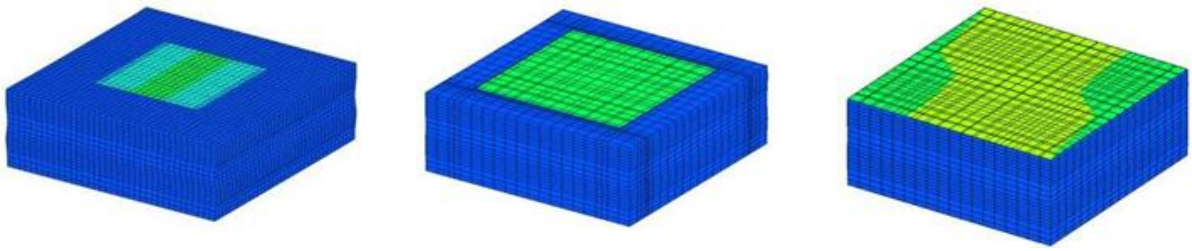

(a) 25% (b) 50% (c) 100%

Figure 2: Bonded portion of STRP: (a) STRP-0; (b) STRP-50; (c) STRP-100

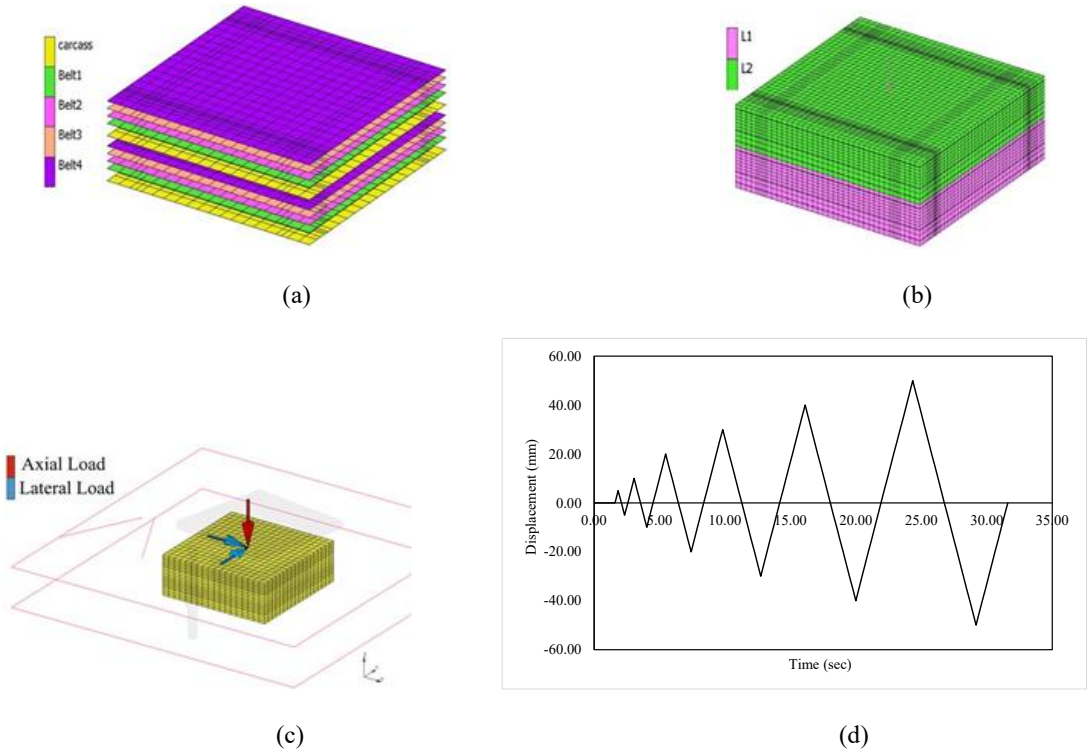

Figure 3: FE modelling of STRP : (a) Position of the embedded rebar components; (b) FE model mesh generation; (c) boundary conditions; (d) Lateral loading pattern

3. FE MODEL VALIDATION

This research presents a comparison examination of the reference model which is founded from Hossain (Hossain et al., 2024) and the finite element model concerning their stiffness data. Figure 4 illustrates that the stiffness patterns for both models exhibit identical behaviours, with the stiffness value initially decreasing with displacement before subsequently increasing at highest % of shear displacement. Despite minor variations in their slope values, the trend behaviour is quite comparable, indicating a substantial degree of congruence. Notwithstanding the variations in loading directions, the stiffness values are approximately equivalent. This verifies that the four models exhibit considerable similarity in patterns while exhibiting modest variations in their values. Consequently, the discrepancies in slope indicate that the two models are closely aligned, affirming that the FE model serves as the reference model due to its ability to accurately represent the initial stiffness response trends.

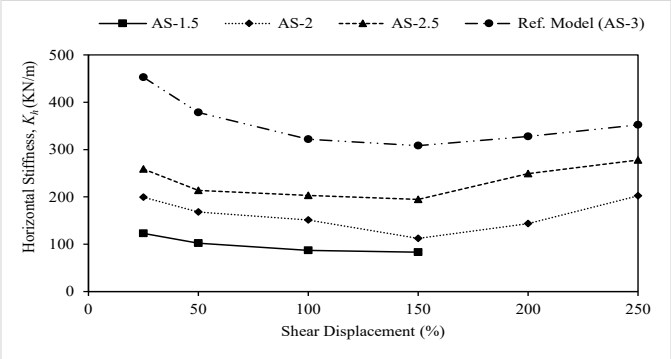

Figure 4: Validation of the FE model against the reference model

4. RESULTS AND DISCUSSIONS

4.1 Force-displacement Relationship

Figure 5 to 7 illustrate the cyclic lateral load response of STRP isolators with variable bond percentages subjected to shear displacements ranging from 25% to 250% where Figure 5 (a) shows Aspect-1 at Y Axis hysteresis curve for 45º Loading; and (b) shows Aspect-1.5 at X Axis hysteresis curve for 45º Loading. Figure 6: (a) shows Aspect-2 at X Axis hysteresis curve for 45º Loading; and (b) shows Aspect-2 at Y Axis hysteresis curve for 45º Loading. Figure 7: (a) shows Aspect-3 at X Axis hysteresis curve for 60º Loading; and (b) shows Aspect-2.5 at Y Axis hysteresis curve for 45º Loading. Though 48mm x 48mm x 24mm, 60mm x 60mm x 24mm and 72mm x 72mm x 72mm isolators demonstrate stability, with no slippage detected in the entirely unbonded STRP isolator. But 72mm x 72mm x 72mm looks more stable. However, Aspect Ratio-1 and Aspect Ratio-1.5 cannot complete a full cycle; they fail before completion and can only withstand a maximum displacement of 150%. However, from Aspect-2, they fulfil the entire cycle. The horizontal stiffness derived from these hysteresis curves are detailed in the subsequent section.

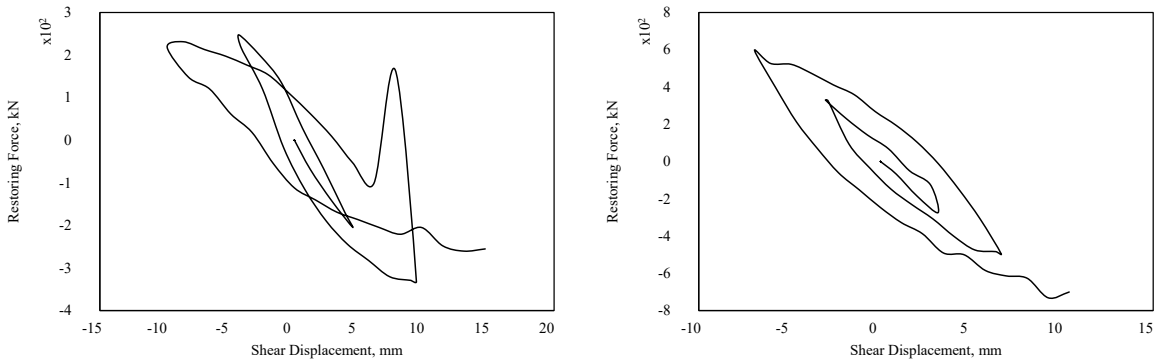

Figure 5: (a) Aspect-1 Y Axis hysteresis curve at 45º Loading; (b) Aspect-1.5 X Axis hysteresis curve at 45º Loading

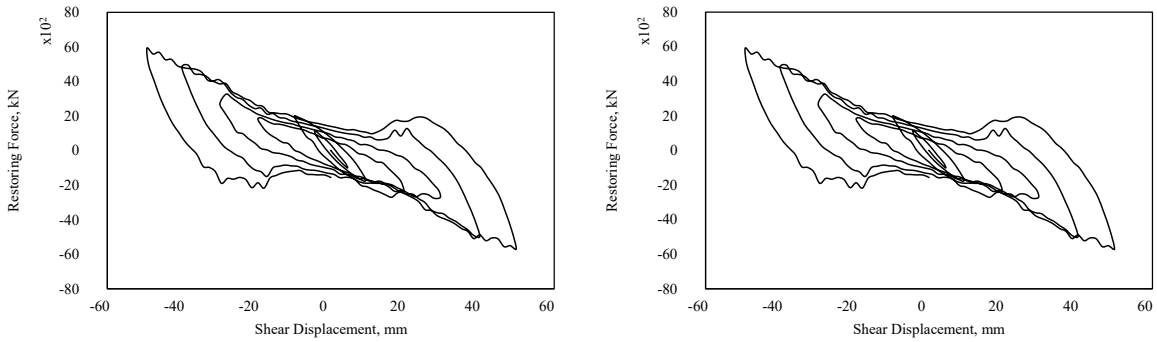

Figure 6: (a) Aspect-2 X Axis hysteresis curve at 45º Loading; (b) Aspect-2 Y Axis hysteresis curve at 45º Loading

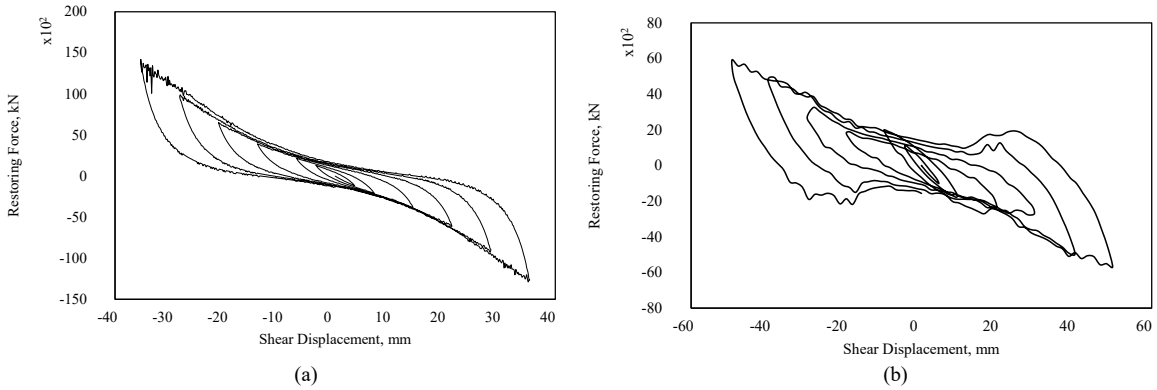

Figure 7: (a) Aspect-3 X Axis hysteresis curve at 60º Loading; (b) Aspect-2.5 Y Axis hysteresis curve at 45º Loading

4.2 Horizontal Stiffness

The horizontal stiffness (K_h) of the STRP isolator is determined using the subsequent formula (ASCE/SEI 7-10, 2010):

$$K_h = \frac{F^+ - F^-}{u^+ - u^-} \quad (1)$$

In this context, F^+ and F^- represent the highest positive and negative forces on the hysteresis curve, corresponding to the maximum positive displacement, u^+, and the maximum negative displacement, u^-, respectively. Tables 4 to 18 present the horizontal stiffness values of STRP isolators. Figure 8 depicts the relationship between maximum and minimum horizontal stiffness concerning aspect ratio. From Table 4 to 18; At an aspect ratio of 1, it is seen that stiffness increases with the increment in loading direction, reaching its peak at a 45° angle of loading. Subsequently, a decline occurs; however, the entirely bonded segment exhibits the maximum value. All aspect ratios of 1.5, 2, 2.5, and 3 exhibit identical patterns. At a 0° orientation, STRP-0 exhibits the lowest stiffness, signifying enhanced flexibility and optimal isolation efficacy. As the bonding area expands, the stiffness value progressively rises until it reaches 75% bonding, at which point the stiffness declines, but it attains its peak at full bonding. Additionally, the lateral stiffness escalates with an increase in lateral displacement, particularly for displacements surpassing 100% shear deformation. The STRP-100 demonstrates superior horizontal rigidity.

Table 4: Horizontal Stiffness for Aspect ratio-1 in loading direction at 0 and 15 degree

Shear Displacement (%)	STRP-0		STRP-25		STRP-50		STRP-75		STRP-100	
	K_h (KN/m)	K_h (KN/m)	K_h (KN/m)	K_h (KN/m)	K_h (KN/m)	K_h (KN/m)	K_h (KN/m)	K_h (KN/m)	K_h (KN/m)	K_h (KN/m)
25	62.27	62.77	63.01	63.13	63.97	64.09	63.22	63.72	64.01	64.19
50	103.89	104.12	104.12	104.24	104.2	104.37	104.27	104.49	104.8	104.89
100	37.24	37.43	37.79	37.93	38.01	38.19	38.1	38.22	38.37	38.58
150	36.78	36.99	37.57	37.63	37.69	37.81	37.8	37.92	38.23	38.33

Table 5: Horizontal Stiffness for Aspect ratio-1 in loading direction at 30 and 45 degree

Shear Displacement (%)	STRP-0		STRP-25		STRP-50		STRP-75		STRP-100	
	K_h (KN/m)	K_h (KN/m)	K_h (KN/m)	K_h (KN/m)	K_h (KN/m)	K_h (KN/m)	K_h (KN/m)	K_h (KN/m)	K_h (KN/m)	K_h (KN/m)
25	63.12	65.41	63.39	65.94	64.23	66.37	63.91	65.77	64.87	66.81
50	104.47	106.68	104.77	107.35	104.98	108.04	105.39	109.06	105.81	109.97
100	37.96	40.62	38.42	41.11	38.59	41.97	38.81	42.17	39.01	43.09
150	37.23	39.85	37.95	40.49	38.12	41.27	37.41	42.44	38.53	43.07

Table 6: Horizontal Stiffness for Aspect ratio-1 in loading direction at 60 and 75 degree

Shear Displacement (%)	STRP-0		STRP-25		STRP-50		STRP-75		STRP-100	
	K_h (KN/m)	K_h (KN/m)	K_h (KN/m)	K_h (KN/m)	K_h (KN/m)	K_h (KN/m)	K_h (KN/m)	K_h (KN/m)	K_h (KN/m)	K_h (KN/m)
25	64.37	64.03	64.79	64.37	65.33	64.72	65.23	64.52	65.86	65.58
50	105.53	105.09	106.97	106.05	107.56	106.78	108.89	106.99	109.02	107.21
100	39.72	38.98	40.37	39.43	40.95	39.97	41.14	40.19	41.26	40.51
150	39.01	38.12	39.65	38.55	40.19	39.15	40.53	39.63	40.98	40.02

Table 7: Horizontal Stiffness for Aspect ratio-1.5 in loading direction at 0 and 15 degree

Shear Displacement (%)	STRP-0		STRP-25		STRP-50		STRP-75		STRP-100	
	K_h (KN/m)	K_h (KN/m)	K_h (KN/m)	K_h (KN/m)	K_h (KN/m)	K_h (KN/m)	K_h (KN/m)	K_h (KN/m)	K_h (KN/m)	K_h (KN/m)
25	122.95	123.31	123.11	123.59	123.75	124.16	124.10	124.83	124.42	125.13
50	102.03	102.44	102.68	103.13	103.01	103.26	104.00	104.36	104.73	105.26
100	86.78	87.12	86.97	87.28	87.77	88.19	88.09	88.90	88.57	89.16
150	83.04	84.17	87.01	87.57	88.02	88.28	88.66	89.21	89.02	89.71

Table 8: Horizontal Stiffness for Aspect ratio-1.5 in loading direction at 30 and 45 degree

Shear Displacement (%)	STRP-0		STRP-25		STRP-50		STRP-75		STRP-100	
	K_h (KN/m)	K_h (KN/m)	K_h (KN/m)	K_h (KN/m)	K_h (KN/m)	K_h (KN/m)	K_h (KN/m)	K_h (KN/m)	K_h (KN/m)	K_h (KN/m)
25	123.95	125.53	124.25	126.12	124.71	126.73	125.55	127.11	126.05	128.44
50	103.07	106.25	103.35	106.9	104.22	107.25	104.78	107.94	105.68	108.83
100	87.78	89.74	88.2	90.32	88.65	90.57	89.58	91.09	90.23	91.81

150	84.88	86.49	88.7	90.97	88.91	91.49	89.90	91.98	90.77	92.41

Table 9: Horizontal Stiffness for Aspect ratio-1.5 in loading direction at 60 and 75 degree

Shear	**STRP-0**		**STRP-25**		**STRP-50**		**STRP-75**		**STRP-100**	
Displacement	K_h	K_h	K_h	K_h	K_h	K_h	K_h	K_h	K_h	K_h
(%)	**(KN/m)**	**(KN/m)**	**(KN/m)**	**(KN/m)**	**(KN/m)**	**(KN/m)**	**(KN/m)**	**(KN/m)**	**(KN/m)**	**(KN/m)**
25	125.01	124.51	125.31	124.93	125.87	125.16	126.34	125.73	127.42	126.46
50	105.68	104.79	105.99	104.98	106.54	105.19	107.05	105.28	108.09	105.89
100	89.03	88.22	89.77	88.71	90.22	89.41	90.92	90.08	91.06	90.53
150	86.19	85.13	90.14	89.30	90.51	89.91	91.01	90.84	91.75	91.08

Table 10: Horizontal Stiffness for Aspect ratio-2 in loading direction at 0 and 15 degree

Shear	**STRP-0**		**STRP-25**		**STRP-50**		**STRP-75**		**STRP-100**	
Displacement	K_h	K_h	K_h	K_h	K_h	K_h	K_h	K_h	K_h	K_h
(%)	**(KN/m)**	**(KN/m)**	**(KN/m)**	**(KN/m)**	**(KN/m)**	**(KN/m)**	**(KN/m)**	**(KN/m)**	**(KN/m)**	**(KN/m)**
25	199.15	200.32	199.37	200.71	200.11	201.1	201.05	201.73	201.77	202.45
50	168.18	169.47	168.73	170.29	169.27	171.29	170.17	171.99	171.19	172.17
100	151.07	152.33	151.71	152.33	152.06	153.19	153.89	154.18	154.45	155.11
150	112.19	113.25	152.12	154.67	153.05	155.5	156.11	157.15	157.10	158.78
200	143.47	144.93	170.0	174.12	171.61	175.62	172.88	176.81	173.33	177.91
250	202.43	203.35	202.98	203.79	203.25	204.27	204.01	204.97	204.68	205.32

Table 11: Horizontal Stiffness for Aspect ratio-2 in loading direction at 30 and 45 degree

Shear	**STRP-0**		**STRP-25**		**STRP-50**		**STRP-75**		**STRP-100**	
Displacement	K_h	K_h	K_h	K_h	K_h	K_h	K_h	K_h	K_h	K_h
(%)	**(KN/m)**	**(KN/m)**	**(KN/m)**	**(KN/m)**	**(KN/m)**	**(KN/m)**	**(KN/m)**	**(KN/m)**	**(KN/m)**	**(KN/m)**
25	201.17	203.88	201.19	204.12	201.85	204.72	202.63	205.1	203.64	205.23
50	170.25	172.77	171.2	173.81	172.01	174.55	172.48	175	173.31	175.43
100	153.34	155.88	153.39	156.06	153.95	156.72	155.15	157.17	156.02	158.64
150	114.51	117.41	155.71	158.04	156.14	158.92	158.21	160.55	159.18	161.03
200	145.77	148.13	175.81	179.15	176.36	179.86	177.12	180.14	178.31	180.03
250	204.32	207.01	204.98	207.79	205.45	208.12	206.09	208.44	206.42	208.94

Table 12: Horizontal Stiffness for Aspect ratio-2 in loading direction at 60 and 75 degree

Shear	**STRP-0**		**STRP-25**		**STRP-50**		**STRP-75**		**STRP-100**	
Displacement	K_h	K_h	K_h	K_h	K_h	K_h	K_h	K_h	K_h	K_h
(%)	**(KN/m)**	**(KN/m)**	**(KN/m)**	**(KN/m)**	**(KN/m)**	**(KN/m)**	**(KN/m)**	**(KN/m)**	**(KN/m)**	**(KN/m)**
25	203.12	202.15	203.17	202.45	201.85	203.12	202.63	203.78	203.64	204.11
50	171.98	171.12	173.01	172.19	172.01	173.33	172.48	173.57	173.31	174.21
100	155.03	154.22	155.56	154.95	153.95	155.61	155.15	156.39	156.02	157.33
150	116.39	115.59	157.13	156.77	156.14	157.13	158.21	159.36	159.18	160.11
200	147.71	146.98	178.05	177.13	176.36	177.77	177.12	178.23	178.31	178.95
250	206.11	205.23	206.79	205.71	205.45	206.42	206.09	207.21	206.42	207.49

Table 13: Horizontal Stiffness for Aspect ratio-2.5 in loading direction at 0 and 15 degree

Shear Displacement (%)	STRP-0		STRP-25		STRP-50		STRP-75		STRP-100	
	K_h (KN/m)	K_h (KN/m)	K_h (KN/m)	K_h (KN/m)	K_h (KN/m)	K_h (KN/m)	K_h (KN/m)	K_h (KN/m)	K_h (KN/m)	K_h (KN/m)
25	259.01	259.33	259.33	259.98	260.1	260.21	260.86	260.88	261.22	261.94
50	213.52	214.17	214.24	215.02	214.98	215.34	215.91	216.36	216.21	216.72
100	202.93	203.07	203.11	203.55	203.23	204.03	203.79	204.78	204.11	205.09
150	194.52	195.13	213.13	213.85	214.09	214.55	214.36	215.07	214.77	214.96
200	249.03	249.97	249.57	250.54	250.02	251	250.62	251.44	251.10	252.01
250	277.75	278.05	278.12	278.36	279.17	279.91	279.85	280.16	280.15	280.93

Table 14: Horizontal Stiffness for Aspect ratio-2.5 in loading direction at 30 and 45 degree

Shear Displacement (%)	STRP-0		STRP-25		STRP-50		STRP-75		STRP-100	
	K_h (KN/m)	K_h (KN/m)	K_h (KN/m)	K_h (KN/m)	K_h (KN/m)	K_h (KN/m)	K_h (KN/m)	K_h (KN/m)	K_h (KN/m)	K_h (KN/m)
25	260.11	261.80	260.65	262.14	261.06	262.46	261.88	263	262.03	263.41
50	215.01	216.42	215.19	216.89	215.60	217.45	216.14	218.02	216.47	218.52
100	203.72	205.01	204.23	205.14	204.25	206.06	205.11	206.37	205.74	206.98
150	195.55	197.10	214.78	220.54	215.04	221.01	215.52	221.49	215.98	222.01
200	250.42	252.12	251.05	252.84	251.97	253.15	252.16	253.04	252.74	253.47
250	278.79	280.09	279.12	280.36	280.10	281.11	280.46	281.78	281.05	282.95

Table 15: Horizontal Stiffness for Aspect ratio-2.5 in loading direction at 60 and 75 degree

Shear Displacement (%)	STRP-0		STRP-25		STRP-50		STRP-75		STRP-100	
	K_h (KN/m)	K_h (KN/m)	K_h (KN/m)	K_h (KN/m)	K_h (KN/m)	K_h (KN/m)	K_h (KN/m)	K_h (KN/m)	K_h (KN/m)	K_h (KN/m)
25	261.15	260.74	261.91	261.30	262.10	261.91	262.31	262.15	262.66	262.38
50	216.01	215.41	216.23	215.92	216.74	216.26	217.48	216.77	217.08	216.93
100	204.46	204.09	205.14	204.52	205.56	205.10	206.12	205.44	206.87	206.02
150	196.65	196.13	216.49	215.87	217.01	216.23	217.17	216.97	217.85	217.08
200	251.49	251.07	252.06	251.42	252.42	252.04	252.89	252.41	253.33	253.11
250	279.56	279.14	280.1	279.75	280.92	280.71	281.48	281.12	282.08	281.74

Table 16: Horizontal Stiffness for Aspect ratio-3 in loading direction at 0 and 15 degree

Shear Displacement (%)	STRP-0		STRP-25		STRP-50		STRP-75		STRP-100	
	K_h (KN/m)	K_h (KN/m)	K_h (KN/m)	K_h (KN/m)	K_h (KN/m)	K_h (KN/m)	K_h (KN/m)	K_h (KN/m)	K_h (KN/m)	K_h (KN/m)
25	452.88	453.31	491.25	490.17	482.47	490.45	475.32	476.03	503.09	503.78
50	378.37	378.45	409.76	410.05	413.11	412.06	416.60	415.83	432.05	432.66
100	321.99	320.12	345.93	346.16	356.47	357.22	377.28	377.54	395.96	394.67
150	308.50	309.01	352.31	354.11	384.57	384.49	404.69	405.51	420.24	421.24
200	327.54	328.06	406.99	416.27	440.49	441.49	461.42	462.02	474.39	476.05
250	352.46	352.98	463.21	463.98	513.88	511.80	526.17	528.89	538.73	545.76

Table 17: Horizontal Stiffness for Aspect ratio-3 in loading direction at 30 and 45 degree

Shear Displacement (%)	STRP-0		STRP-25		STRP-50		STRP-75		STRP-100	
	K_h (KN/m)	K_h (KN/m)	K_h (KN/m)	K_h (KN/m)	K_h (KN/m)	K_h (KN/m)	K_h (KN/m)	K_h (KN/m)	K_h (KN/m)	K_h (KN/m)
25	454.11	456.05	486.51	483.55	491.77	496	476.78	479.80	503.98	508.42
50	378.96	380.14	410.55	414.13	410.29	416.22	414.85	416.79	432.91	436.36
100	319.96	318.84	346.79	349.01	358.98	363.33	377.75	391.46	392.79	402.76
150	309.49	310.76	360.64	368.88	384.35	387.19	406.87	442.11	422.05	449.14
200	329.14	331.79	415.89	418.13	444.23	449.01	463.14	500.12	476.96	545.53
250	353.86	358.62	464.17	467.51	509.12	508.65	531.12	575.54	551.80	639.3

Table 18: Horizontal Stiffness for Aspect ratio-3 in loading direction at 60 and 75 degree

Shear Displacement (%)	STRP-0		STRP-25		STRP-50		STRP-75		STRP-100	
	K_h (KN/m)	K_h (KN/m)	K_h (KN/m)	K_h (KN/m)	K_h (KN/m)	K_h (KN/m)	K_h (KN/m)	K_h (KN/m)	K_h (KN/m)	K_h (KN/m)
25	455.1	454.77	482.2	484.46	493.7	492.78	477.9	476.88	504.3	504.14
50	379.3	379.19	411.2	411.02	408.0	409.31	413.7	413.98	433.3	433.06
100	318.2	319.07	347.6	347.09	361.9	360.59	378.0	377.9	391.8	392.12
150	310.2	310.01	367.6	365.29	384.1	384.21	408.2	407.22	423.8	423.01
200	330.9	330.13	415.0	415.42	447.3	445.98	464.6	463.87	478.8	477.85
250	356.0	354.65	465.6	465	506.3	507.81	534.8	533.54	558.1	555.75

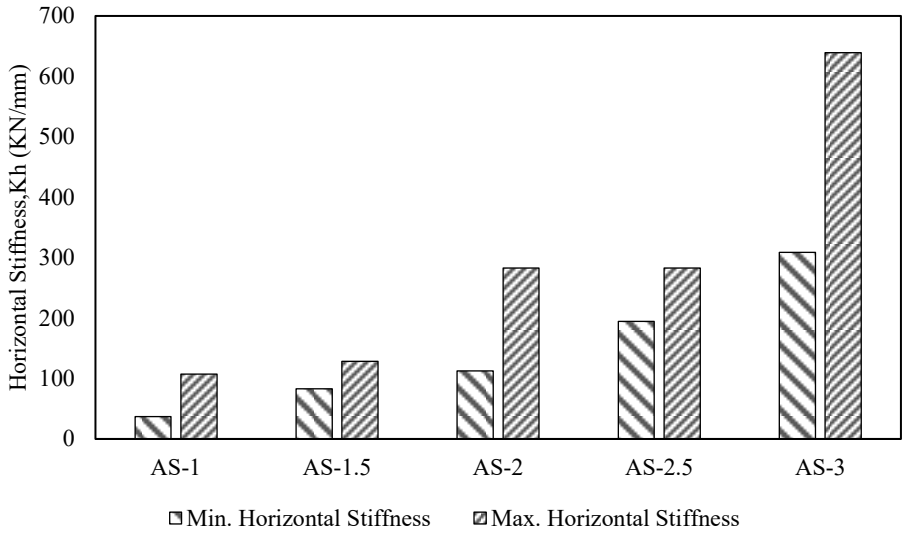

Figure 8: Highest and Lowest Horizontal Stiffness according to Aspect ratio for STRP

5. CONCLUSIONS

This study has examined the lateral load performance of STRP isolators with differing bonding areas between the isolator and structural levels under cyclic bi-directional lateral stress. Square and cuboidal isolators are analysed under cyclic loading orientations ranging from 0° to 75° in 15° increments, with aspect ratios of 1, 1.5, 2, 2.5, and 3 compared. The principal conclusions are as follows:

- STRP-0 (unbonded) has shown the least stiffness and fully bonded has shown highest stiffness. Though, unbonded can show slippage but fully bonded can be fractured due to its over stiffness.
- For aspect ratios of 1, 1.5, 2, 2.5, and 3, lateral stiffness increases with the increment in loading angle, reaching its peak at 45 degrees. It then decreases at 60 degrees but climbs again at 75

degrees, although it does not exceed the stiffness established at 45 degrees. However, aspect ratios of 1 and 1.5 exhibit a total displacement of 150%, whilst all other aspect ratios have a lateral displacement of 250%.

- The minimum stiffness recorded at an aspect ratio of 1 for a 0-degree loading direction in an unbonded pad isolator is 36.78 KN/m, while the maximum stiffness is observed at an aspect ratio of 3 for a 45-degree loading direction at 250% displacement, measuring 639.3 KN/m.
- Maximum stiffness has been found for aspect-1 to 3, 109.97 KN/m, 128.44 KN/m, 208.94 KN/m, 282.95 KN/m and 639.3 KN/m, respectively. On the other hand, lowest has been found for same scenario, 36.78 KN/m, 83.04 KN/m, 112.19 KN/m, 194.52 KN/m and 308.50 KN/m, respectively.
- From aspect ratio-1 to 1.5, maximum 16.79% lateral stiffness has been increased, from 1.5 to 2, 62.67% stiffness has been increased. From aspect ratio-2 to 2.5, the number of enhancements has dropped than previous, maximum 35.42% stiffness has been increased. From aspect ratio-2.5 to 3, a big jump has been found, maximum 125.94% have increased here.
- Although Aspect Ratio-1 has the lowest performance, it lacks stability for the structure; therefore, Aspect-3 performs significantly better in this context.
- These findings offer direction for the selection of STRP isolators in structural applications, contingent upon the required stiffness and flexibility.

DECLARATION OF USE OF AI

The authors state that QuillBot, an AI-assisted tool, was only utilized for language editing and paraphrasing in order to enhance the manuscript's readability, grammar, and clarity. The creation of scientific content, data analysis, result interpretation, and study methods were not handled by the AI tool. The authors are solely responsible for all scientific content, analyses, and findings.

REFERENCES

Marc-Mentat, MSC. (2018). Theory and user information, Vol. A, Santa Ana, CA: MSC Software Corporation.

Zisan, M.B., & Igarashi, A. (2021). Lateral load performance and seismic demand of unbonded scrap tire rubber pad base isolators. *Earthquake Engineering and Engineering Vibration*, 803–821.

Kelly, J.M. (1999). Analysis of Fiber-Reinforced Elastomeric Isolators. *Journal of Seismology and Earthquake Engineering.*, 19-34.

Mashiri, M.S., Vinod, J.S., Sheikh, M.N., & Tsang, H.H. (2015). Shear strength and dilatancy behaviour of sand–tyre chip mixtures. *Soils and Foundations*, 517-528.

Hossain, M.M., Zisan, M.B., Maher, S.K., & Abdullah, N. (2024). Effect of Loading Directionality On Seismic Behavior Of Partially Bonded Square-Shaped Scrap Tire Rubber Pad Isolator. *7th Internation Conference on Advances in Civil Engineering (ICACE-2024)* (pp. 2471-2478). Chattogram: Dept. of Civil Engineering, Chittagong University of Engineering & Technology, Chattogram, Bangladesh.

Mishra, H. K. (2012). *Experimental and Analytical Studies on Scrap Tire Rubber Pads for Application to Seismic Isolation of Structures.* Kyoto,Japan: Kyoto University.

Pan, P., Zamfirescu, D., Nakashima, M., Nakayasu, N., & Kashiwa, H. (2005). Base-Isolation Design Practice In Japan: Introduction To The Post-Kobe Approach. *Journal of Earthquake Engineering, 9(1)*, 147–171.

Nishi, T., Suzuki, S., Aoki, M., Sawada, T., & Fukuda, S. (2019). International investigation of shear displacement capacity of various elastomeric seismic-protection isolators for buildings. *Journal of Rubber Research*, 33–41.

Zisan, M.B., & Igarashi, A. (2022). A Hysteresis Force Model For Unbonded Scrap Tire Rubber Pad Isolators. *3rd International Conference on Natural Hazards & Infrastructure (ICONHIC2022).* Athens, Greece: ICONHIC2022.